

Molded Geometry and Viscoelastic Behavior of Film Insert Molded Parts

Seong Yun Kim,¹ Sung Ho Kim,¹ Hwa Jin Oh,¹ Seung Hwan Lee,¹ Soo Jin Baek,¹ Jae Ryouun Youn,¹ Sung Hee Lee,² Sun-Woo Kim³

¹Department of Materials Science and Engineering, Research Institute of Advanced Materials (RIAM), Seoul National University, Sillim-Dong, Gwanak-Gu, Seoul, 151-744 Korea

²Precision Molds and Dies Team, Korea Institute of Industrial Technology, Songdo-Dong, Yeonsu-Gu, Incheon, 406-840, Korea

³Min Sung Precision Co. Ltd., Samjung-Dong, Ojung-Gu, Buchon, Gyeonggi-do, 421-808, Korea

Received 26 April 2008; accepted 18 August 2008

DOI 10.1002/app.29121

Published online 12 October 2008 in Wiley InterScience (www.interscience.wiley.com).

ABSTRACT: Virgin injection-molded tensile specimens without any inserted film and four kinds of film insert molded (FIM) tensile specimens were prepared. They were annealed at 80°C to investigate the effect of residual stresses and thermal shrinkage of the inserted film on thermal deformation of tensile specimens. The FIM specimens with the unannealed film were bent after ejection in such a way that the film side was protruded and the warpage was reversed gradually during annealing and the film side was intruded. Warpage of the FIM specimen with the film annealed at 80°C for 20 days was not reversed during annealing. Processing of the FIM specimens have been modeled numerically to predict thermoviscoelastic deformation of the part and to understand the warpage reversal phenomenon (WRP).

Nonisothermal three-dimensional flow analysis was carried out for filling, packing, and cooling stages. The flow analysis results were transported to a finite element stress analysis program for prediction of deformation of the FIM part. The WRP was caused by the combined effect of thermal shrinkage of the inserted film and relaxation of residual stresses in the FIM specimen during annealing. It is expected that this study will contribute towards the improvement of the FIM product quality and prevention of large viscoelastic deformation of the molded part. © 2008 Wiley Periodicals, Inc. *J Appl Polym Sci* 111: 642–650, 2009

Key words: annealing; films; injection molding; viscoelastic properties

INTRODUCTION

Film insert molding (FIM) is an injection-molding method in which molten polymer is filled into the cavity after a film is attached to one side of the mold walls. Surface quality of the product can be improved by the inserted film, e.g., durability, esthetic appearance, surface design and color, etc. Moreover, the injected hot resin may wet and remelt the film partially, which would enhance adhesion between the film and the substrate after the part is cooled.^{1–4} FIM is an effective technique in the aspect of product cost and manufacturing time because the ejected product can be used without additional bonding or decorating processes like screen printing, spray painting, heat-induced labeling, etc. The FIM method has been widely applied lately to various

injection molded products such as automotive interior parts, cellular phone cases, logo design of plastic products, etc.

However, washing off of printed ink, wrinkling of the film, and other problems related to product appearance are sometimes observed. In particular, warpage and nonuniform shrinkage of the product can occur due to asymmetric residual stress distribution which is mainly developed by nonuniform heat transfer. The inserted film has different thermal conductivity compared with the injected polymer resin in most cases and causes the nonuniform heat transfer.⁵ Although there are many studies reported on the warpage and shrinkage of injection molded parts,^{6–12} investigations on the warpage of FIM products are still in just a rudimentary stage. Therefore, it is necessary to survey the residual stress distribution and viscoelastic deformation of FIM parts, which can influence on their warpage.

Numerical analysis is important to understand the processing procedure and physical properties of final product beforehand. Numerical flow analysis of FIM can be performed by using a three-dimensional finite element analysis with the capability of part

Correspondence to: J. R. Youn (jaeryoun@snu.ac.kr).

Contract grant sponsor: Korea Science and Engineering Foundation (through the Applied Rheology Center (ARC) at Korea University).

TABLE I
Injection Molding Conditions

	Film annealing	Mold temperature (°C)		Melt temperature (°C)	Packing pressure (MPa)	Injection speed (mm/s)
		Resin side ^a	Film side			
VITS	No	40	43	250	30	40
FITS1	No	40	43	250	30	40
FITS2	No	10	43	250	30	40
AFITS2	Yes	10	43	250	30	40

^a At mold temperature, resin side means that the mold temperature at the interface between injected resin and mold cavity and film side also represents that the mold temperature at the interface between inserted film and mold cavity. VITS, FITS, and AFITS represent virgin injection molded tensile specimen, film insert molded tensile specimen, and annealed film insert molded tensile specimen, respectively.

insert in Moldflow, a commercially available code for injection molding. However, residual stresses in the FIM part are obtained only in the substrate domain after being ejected from the mold cavity by assuming isotropic elastic deformation. It is not possible to calculate residual stresses in the film domain since the interfacial bonding between the two domains cannot be taken into account in the molding simulation software. Time-dependent viscoelastic deformation of the part after ejection can be predicted by using a numerical stress analysis program.¹³

In this study, FIM tensile specimens were prepared to investigate the warpage of FIM parts after ejection from the cavity. Virgin injection-molded tensile specimens without inserted film were also prepared to compare them with FIM tensile specimens. After ejection, four different kinds of tensile specimens were annealed to investigate their thermoviscoelastic deformation, and it was observed that the FIM one was warped in the opposite direction after annealing. The peculiar observation, namely, "warpage reversal phenomenon (WRP)" was investigated. Full three-dimensional molding and structural analyses were carried out to understand the WRP. For calculation of residual stresses and viscoelastic deformation of FIM specimens, a commercial stress analysis code, ABAQUS, was utilized. Therefore, objective of this study is to comprehend and predict the WRP which can occur in FIM practice and to minimize long-term viscoelastic deformation or possible fracture of the FIM product.

EXPERIMENTS

Materials

The film employed for molding of the FIM specimen has a laminated structure that consists of acrylonitrile butadiene styrene (ABS) substrate and polymethylmetacrylate (PMMA) film. Thickness of the PMMA layer was 0.05 mm and that of the ABS layer was 0.45 mm when supplied by the manufacturer (Nissha printing Co., Ltd., Japan). It is expected that

biaxial molecular orientation and residual stresses are developed in the film during the manufacturing process. The polymeric resin used for injection was a blend of polycarbonate (PC) and ABS (HP-1000X, Cheil industries inc., Korea).

Characterization of materials

Dimensions of the unannealed film and the annealed film treated at 80°C were measured. Linear thermal expansion coefficient, α , of the film was determined by the following equation.

$$\alpha = \frac{\Delta l}{l_0 \Delta T} \quad (1)$$

where Δl is deformed length, l_0 is initial length, and ΔT is temperature difference. For modeling of viscoelastic properties of materials, relaxation moduli of the film, and substrate were measured by using the dynamic mechanical analysis (DMA 2980, TA instrument, USA). To obtain rheological property of the substrate at high shear strain rate region, a capillary rheometer (Rheograph 6000, Göttfert, Germany) equipped with a single bore die whose diameter is 1 mm was used in the shear strain rate region from 100 s⁻¹ to 2000 s⁻¹ at 250°C and 260°C, respectively.

Film insert injection molding

The film was annealed at 80°C for 20 days to minimize the effects of thermal shrinkage and residual stresses on the warpage of film insert injection molded parts. The PC/ABS blend was dried at 80°C *in vacuo* for 4 h before injection molding to minimize the effect of moisture. The unannealed or annealed film was attached to one side of the mold wall before injection of the resin. The polymer blend was injected into a dog bone shaped cavity by using an injection molding machine (Engel, Germany). The molding conditions were summarized in Table I. The difference between FITS1 and FITS2 is just inclusion of black colorant or not, but the specimens were separated because the fact might influence on

warpage of specimens. After ejection, the molded specimens were annealed in a convection oven at 80°C and for various time periods of 10, 20, 30 min and 2 h to evaluate viscoelastic deformation of the tensile specimens. The warpage was measured before and after annealing by scanning the specimens with a scanner (Hewlett-Packard, USA).

Measurement of residual stresses

There are many measurement methods to determine residual stresses. The layer-removal method which was developed by Treuting and Read¹⁴ is one of the most commonly used destructive methods, but is limited to the measurement of residual stresses in flat plates. It is impossible to apply the technique to an object with complex geometry.^{14–17} On the other hand, the hole-drilling method is applicable to a small area of an object, or an object with a complex geometry, and so this study employed the hole-drilling method to evaluate residual stress in curved and flat films. The hole-drilling method is a semides- tructive residual stress measurement technique which was first proposed by Mathar.¹⁸ Introduction of a hole into a stressed body relaxes the stress at the location. The removal of stressed material causes localized stress relaxation and deformation around the hole. Strain distribution caused by the deformation can be measured by using a specially designed strain gauge rosette. The procedure is relatively simple and has been standardized as depicted in ASTM Standard Procedure E837.

The experimental set-up employed previously^{19,20} for the hole-drilling method was used. A special three-element strain gauge rosette (062UL type, Measurement Group, USA) was installed on the surface of the films at the point where residual stresses were to be determined. Figure 1 shows the annealed film with the attached rosette where the residual stress distribution was measured with respect to depth by using the hole drilling method. A precision milling guide (RS-200, Measurement Group, USA) was attached to the specimen and centered accurately over a drilling target in the rosette. One can measure the induced strain at each drilling step and consider the relationship between the strain and principal stresses to determine the level of residual stresses.^{21,22} In this study, the integral method was used to measure the residual stresses because it was appropriate to evaluate the residual stress variation for each increment in thickness direction during the incremental hole-drilling measurement.^{23–26}

The elastic strain, ϵ_{rr} , was measured by the rosette at the periphery of the hole and is related to the principal stresses by the following equation:

$$\epsilon_{rr} = (\bar{A} + \bar{B} \cos 2\beta)\alpha_{\max} + (\bar{A} - \bar{B} \cos 2\beta)\sigma_{\min}, \quad (2)$$

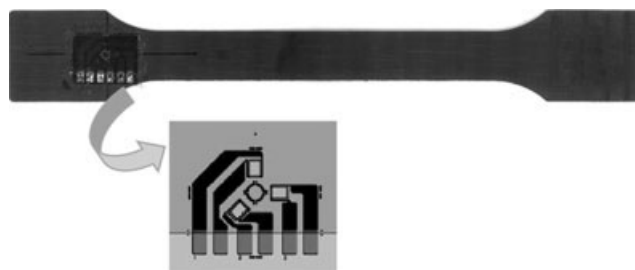


Figure 1 An annealed film with a rosette attached and the rosette (062UL type) employed in the experiment.

$$\bar{A} = -\frac{\bar{a}(1+\nu)}{2E}, \quad \bar{B} = -\frac{\bar{b}}{2E}, \quad (3)$$

where σ_{\max} and σ_{\min} are principal stresses, β is an angle measured counterclockwise from the maximum principal stress direction to the axis of the strain gauge, \bar{A} and \bar{B} are calibration constants, \bar{a} and \bar{b} are dimensionless constants, E is Young's modulus, and ν is Poisson's ratio. Magnitude and direction of the two principal stresses are obtained in terms of the measured strains.

$$\sigma_{\max}, \sigma_{\min} = \frac{\epsilon_1 + \epsilon_3}{4\bar{A}} \mp \frac{\sqrt{(2\epsilon_2 - \epsilon_1 - \epsilon_3)^3 + (\epsilon_1 - \epsilon_3)^2}}{4\bar{B}} \quad (4)$$

$$\beta = \frac{1}{2} \tan^{-1} \left(\frac{2\epsilon_2 - \epsilon_1 - \epsilon_3}{\epsilon_1 - \epsilon_3} \right) \quad (5)$$

where ϵ_1 , ϵ_2 , and ϵ_3 are relaxed strains measured by the strain gauge.^{18,21,22,27–29}

NUMERICAL SIMULATION

The FIM part consists of film and substrate materials and it is not possible to predict melt flow into the cavity and development of residual stresses of the part with two-dimensional numerical analysis. Three-dimensional simulation of the molding process is required especially for numerical analysis of the viscoelastic deformation of the FIM part. A mesh generating program, HyperMesh, was employed to generate two-dimensional finite element meshes for film and substrate domains of the tensile specimen. The two-dimensional finite elements were created separately for film and substrate domains and three-dimensional finite elements were created after they were imported to Moldflow and combined together.

Numerical analysis of injection molding

A set of unified governing equations based upon the generalized Hele-Shaw model of a compressible

viscous fluid is used for nonisothermal analysis of the filling and postfilling stages. Three dimensional flow analysis is performed by assuming that rheological behavior of the polymeric melt follows the modified Cross model with the Williams-Landel-Ferry (WLF) equation,^{30,31}

$$\eta = \frac{\eta_0}{1 + \left(\frac{\eta_0 \dot{\gamma}}{\tau^*}\right)^{(1-n)}} \quad (6)$$

$$\log \frac{\eta_0 \theta^* \rho^*}{\eta^* \theta \rho} = \frac{-C_1(\theta - \theta^*)}{C_2 + (\theta - \theta^*)}$$

where, η is viscosity, η_0 is zero shear rate viscosity, $\dot{\gamma}$ is shear rate, τ^* is shear stress at the transition between Newtonian and power law behavior, η^* is viscosity at reference temperature, ρ is density, ρ^* is density at reference temperature, θ is temperature and θ^* is reference temperature. The change in the ratio, $\theta^* \rho^* / \theta \rho$, is small and often ignored. Typically θ^* is chosen as the glass transition and $C_1 = 17.44$ and $C_2 = 51.6$ K for many polymers. Convective heat transfer by the cooling liquid, viscous heating during both filling and postfilling stages, and heat conduction through the mold-polymer interface are accounted for in the thermal analysis. The PVT relationship is represented by the modified Tait equation. The coupled thermal and flow fields are solved with the control-volume approach to handle automatic melt-front advancement by using a hybrid FEM/FDM scheme. An implicit numerical scheme is employed to solve the discretized energy equation.³²

Since the PMMA layer is thin enough, the laminated film was considered as a homogeneous film by neglecting the PMMA layer. Properties of ABS (techno ABS 545, Techno polymer) were employed for properties of the film. In Figure 2, the viscosity of the PC/ABS blend is shown with respect to the shear strain rate and both data were in good agreement each other. Properties of a polymer resin (Lupoy HR5007AB, LG Chemical) whose rheological property was the same as that of the substrate resin were selected as properties of the injected resin for flow analysis. The selected material properties for

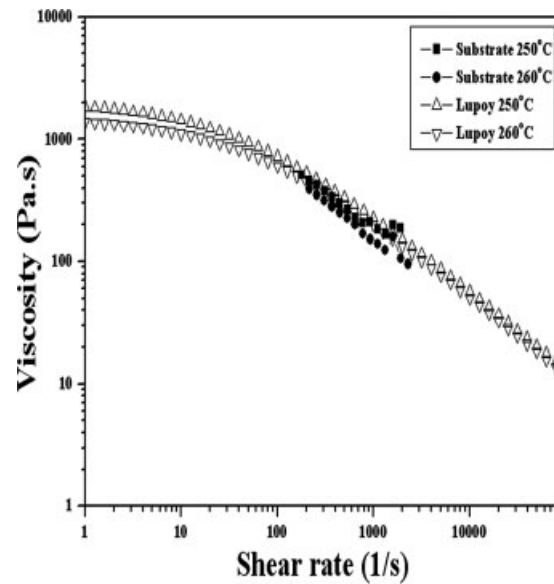


Figure 2 Viscosity variation of the substrate resin and Lupoy HR5007AB with respect to shear strain rate at 250°C and 260°C.

the polymer resin and film are summarized in Table II, and the numerical molding conditions are same with the experimental ones, in Table I. At the end of the flow analysis, the output data was exported to the stress analysis program and the interface between the film and the substrate was joined. The in-mold condition of the part was exported to the stress simulation code and used as the initial condition for structural analysis of the FIM part.

Viscoelastic stress analysis

Residual stresses and deformation of the injection molded part is analyzed by applying elastic properties of the solid polymer right after ejection from the mold cavity. However, various material properties can be applied to the part for prediction of the stress relaxation with respect to time and temperature, e.g., elastoplastic, hyperelastic, plastic, and viscoelastic properties. In particular, Viscoelastic property is

TABLE II
Material properties of the film and resin for numerical simulation

	Film (Techno ABS545)	Resin (Lupoy HR 5007AB)
Elastic modulus (MPa)	2240	2780
Poisson's ratio	0.392	0.23
Thermal conductivity (W/m.°C)	0.116 (at 75°C, temperature dependent)	0.21 (at 79°C, temperature dependent)
Thermal expansion coefficient (K ⁻¹)	8 × 10 ⁻⁵ (or -4.2 × 10 ⁻⁵) ^a	6.7 × 10 ⁻⁵
Specific heat (J/kg.°C)	2202 (at 200°C, temperature dependent)	2205 (at 265°C, temperature dependent)
Solid density (kg/m ³)	1054.1	1136.7
Melt density (kg/m ³)	943.9	1003.6

^a The reason why two kind of thermal expansion coefficients of the film were used was explained at section Viscoelastic stress analysis.

important to predict time-dependent deformation of polymeric parts which are exposed to various environmental conditions. The structural analysis was performed to calculate residual stress development at the instant of ejection and to evaluate long-term thermoviscoelastic deformation. For long-term behavior of the polymers, it is assumed that the polymer material is transversely isotropic with viscoelastic stress-strain behavior, where the dependence of material behavior on temperature is accounted for though the assumption of thermorheological simplicity.

The constitutive equation for the linear viscoelastic material in the thermal stress analysis is the generalized Kelvin model that is represented by hereditary integrals and the effect of temperature is considered^{33,34} by the following equation.

$$\tau(t) = G_0(\theta) \left(\gamma - \int_0^t \dot{g}_R(\xi(s)) \gamma(t-s) ds \right) \quad (7)$$

where the instantaneous shear modulus G_0 is temperature-dependent and γ is the shear strain.

$$\dot{g}_R(\xi) = dg_R/d\xi, \quad g_R(t) = G_R/G_0 \quad (8)$$

where $G_R(t)$ is the time-dependent shear relaxation modulus that characterizes the material's response and $g_R(t)$ is dimensionless relaxation modulus. $\xi(t)$ is reduced time defined by the following equation.

$$\xi(t) = \int_0^t \frac{ds}{A(\theta(s))} \quad (9)$$

where $A(\theta(t))$ is a shift function at time t . Temperature dependence of the reduced time is usually referred to as the thermorheologically simple (TRS) temperature dependence. The shift function is often approximated by the WLF form.

$$\log(A) = \frac{-C'_1(\theta - \theta^*)}{C'_2 + (\theta - \theta^*)} \quad (10)$$

where θ^* is the reference temperature at which the relaxation data are provided and C'_1 and C'_2 are calibration constants obtained at the temperature.

$$C'_1 = \frac{C_1^g}{1(\theta^* - \theta_g)/C_2^g}, \quad C'_2 = C_2^g + \theta^* - \theta_g \quad (11)$$

where C_1^g and C_2^g are universal constants, which are 17.4 and 51.6 K, respectively. Normalized shear relaxation moduli measured for the substrate and the film are shown in Figure 3 and used for the viscoelastic stress analysis.

As mentioned above, the ejection step was dealt with by solving an elastic problem when fixed boundary conditions are removed suddenly and the viscoelastic deformation step was performed by

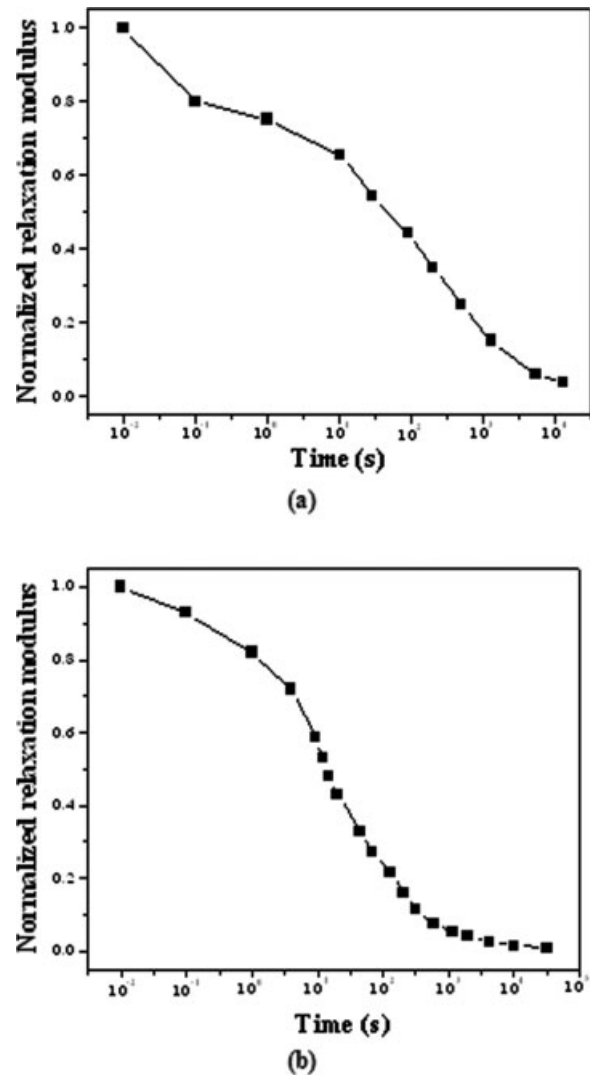


Figure 3 Normalized relaxation moduli measured: (a) film and (b) substrate.

assuming that the part was kept at 80°C for 30 min. Thermal expansion coefficient of the annealed film was chosen as that of the ABS, $8 \times 10^{-5} \text{ K}^{-1}$. However, thermal expansion coefficient of the unannealed film was determined by experiments as $-4.2 \times 10^{-5} \text{ K}^{-1}$ for numerical modeling of the annealing until the first heating step is over because the film undergoes contraction due to irreversible relaxation of the molecular orientation which had been developed by biaxial drawing during film extrusion. Figure 4 shows the dimensional change of the film annealed at 80°C with respect to increasing annealing time. From the result, the thermal expansion coefficient was obtained experimentally. After the first heating step, thermal expansion coefficient of the unannealed film was given by that of the ABS ($8 \times 10^{-5} \text{ K}^{-1}$) because it would have the thermal expansion coefficient of the annealed film. Naturally, the annealed film undergoes negligible relaxation of

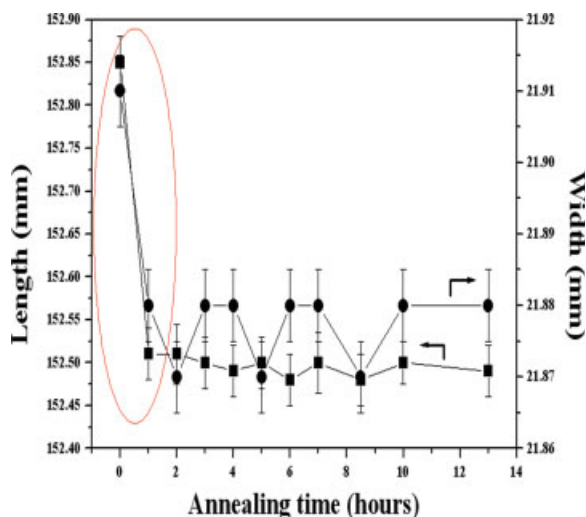


Figure 4 Variation in the dimension of the film annealed at 80°C with respect to increasing annealing time. [Color figure can be viewed in the online issue, which is available at www.interscience.wiley.com.]

the molecular orientation during heat treatment of the FIM part and has constant thermal expansion coefficient for the entire heating steps.

RESULTS AND DISCUSSION

Warpage of VITS and FITS1 specimens before and after annealing are shown in Figure 5(a–d). The molded VITS specimens had little warpage before or after annealing as shown in (a) and (b) because the specimens were molded without the film while the

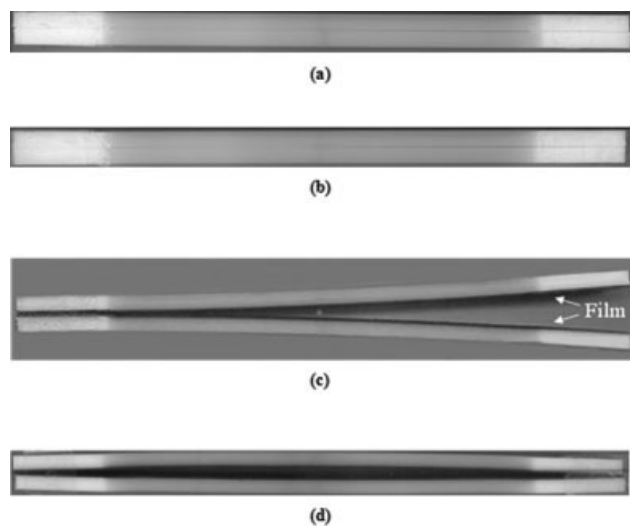


Figure 5 Warpage of molded specimens without the film (VITS) and with the inserted film (FITS1): (a) VITS before annealing, (b) VITS annealed at 80°C for 2 h, (c) FITS1 before annealing, and (d) FITS1 annealed at 80°C for 2 h.

same temperature was maintained at both core and cavity sides of the cavity. On the other hand, FITS1 specimen in (c) was bent after ejection such that the film side was protruded because shrinkage of the solid film side was lower than that of the other side where polymer melt had been solidified by the cold surface of the mold. Figure 5(d) showed that FITS1 specimen annealed at 80°C for 2 h was bent such that the opposite side of the film was protruded. This interesting behavior is named “WRP”. The WRP occurred naturally due to the inserted film, in particular, because of thermal shrinkage of the film and relaxation of residual stresses in the entire part. To begin with, it is necessary to investigate thermal behavior of the film for proof of the discussion.

The residual stress distribution in the unannealed film and the film annealed at 80°C is shown with respect to the depth in Figure 6. The residual stress distribution of the unannealed film was varied as compression, tension, compression, and tension from the PMMA layer to the ABS layer, but that of the film annealed for 12 h was varied as tension and compression and that of the film annealed for 7 days was almost similar with that of the film annealed for 12 h. The residual stresses in the unannealed film had been relaxed during annealing and the residual stress distribution in the film was newly developed by the difference in thermal expansion coefficient between PMMA and ABS layers. As shown in Figure 4, thermal shrinkage of the film was observed in the early stage of annealing and maybe due to the relaxation of molecular orientation generated by the biaxial drawing of the film performed in typical film manufacturing processes.

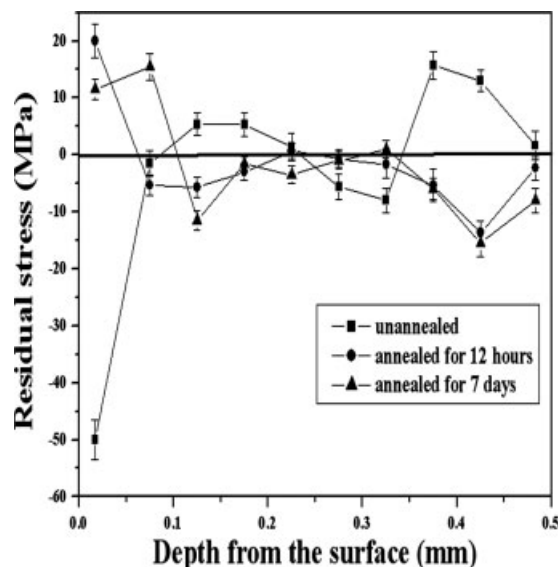


Figure 6 Residual stress distribution with respect to depth of the unannealed film and the annealed film treated at 80°C for 12 h or 7 days.

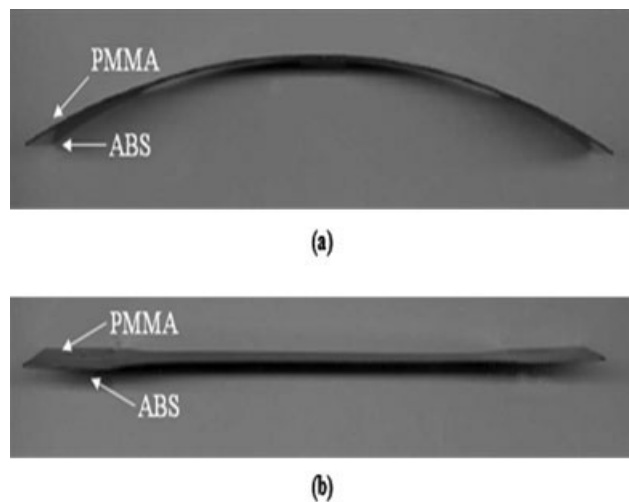


Figure 7 Side view of the film: (a) original shape of the unannealed film and (b) changed shape of the film annealed for 7 days.

The pristine and deformed shapes of the film after annealing at 80°C for 20 days are shown in Figure 7(a,b). The pristine film was bent such that the thin PMMA layer was protruded as shown in Figure 7(a) and compressive residual stresses were present in the PMMA layer. The film will be flattened by the relaxation of residual stresses and different thermal shrinkage of the PMMA and ABS layers when it is heated. As shown in Figure 7(b), the film became flat after annealing and the residual stress in the PMMA layer was changed from compressive residual stress to tensile residual stress. It is expected that the thermal shrinkage of the film will impose larger effect on the deformation of the film during annealing than the relaxation of residual stresses.

As mentioned previously, Treuting et al.¹⁴ suggested the layer removal method for measuring residual stresses in a thin plate made of linear elastic and isotropic material. As a thin layer is removed from the surface, the part is deformed to recover its equilibrium from the unbalanced residual stress distribution due to the layer removal. A precision experimental setup and standard experimental procedure are needed to measure the residual stresses accurately. To investigate the mode of residual stress distribution such as tensile or compressive in the film layer of the FIM part, the inserted film was roughly peeled off from the FITS1 specimen



Figure 8 Side view of FITS1 after the film is roughly peeled off after ejection.

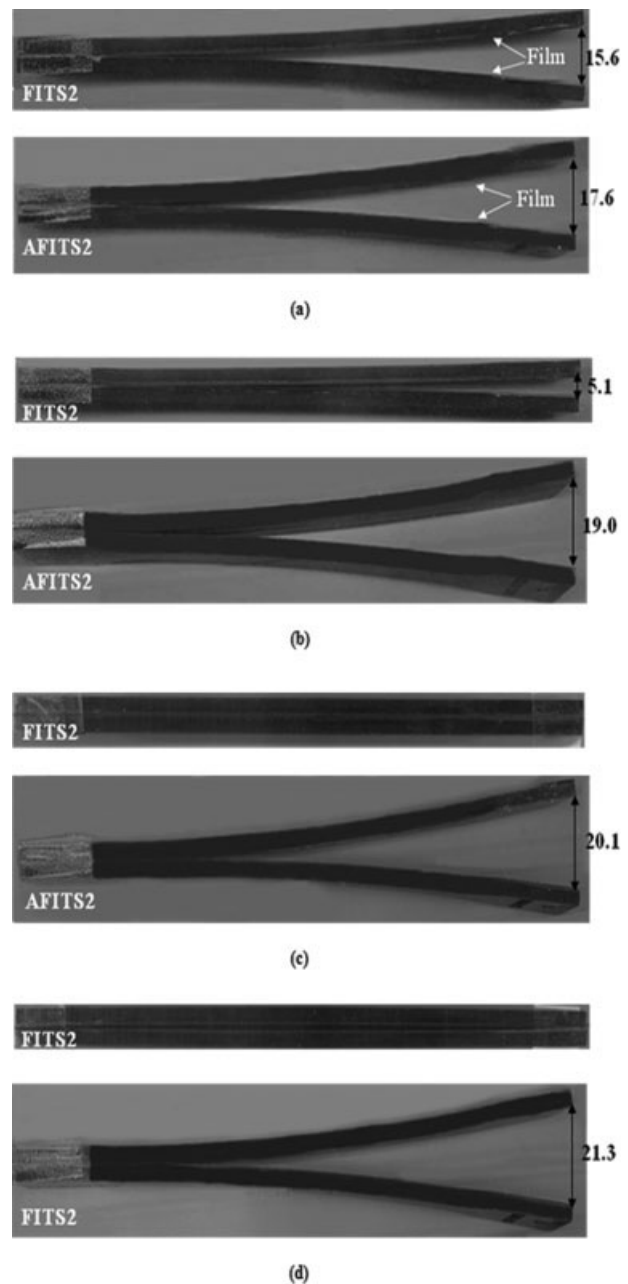


Figure 9 Warpage of FITS2 and AFITS2 specimens observed after ejection and annealing at 80°C with increasing annealing time: (a) after ejection, (b) for 10 min, (c) for 20 min, and (d) for 30 min.

right after ejection. The peeled specimen is exhibited in Figure 8 and it was observed that the specimen was bent in the opposite direction such that the surface of the removed film was intruded slightly. This result meant that a large amount of compressive residual stress had been developed in the film during molding and that the residual stress distribution of the unannealed film had been changed from compression, tension, compression, and tension modes

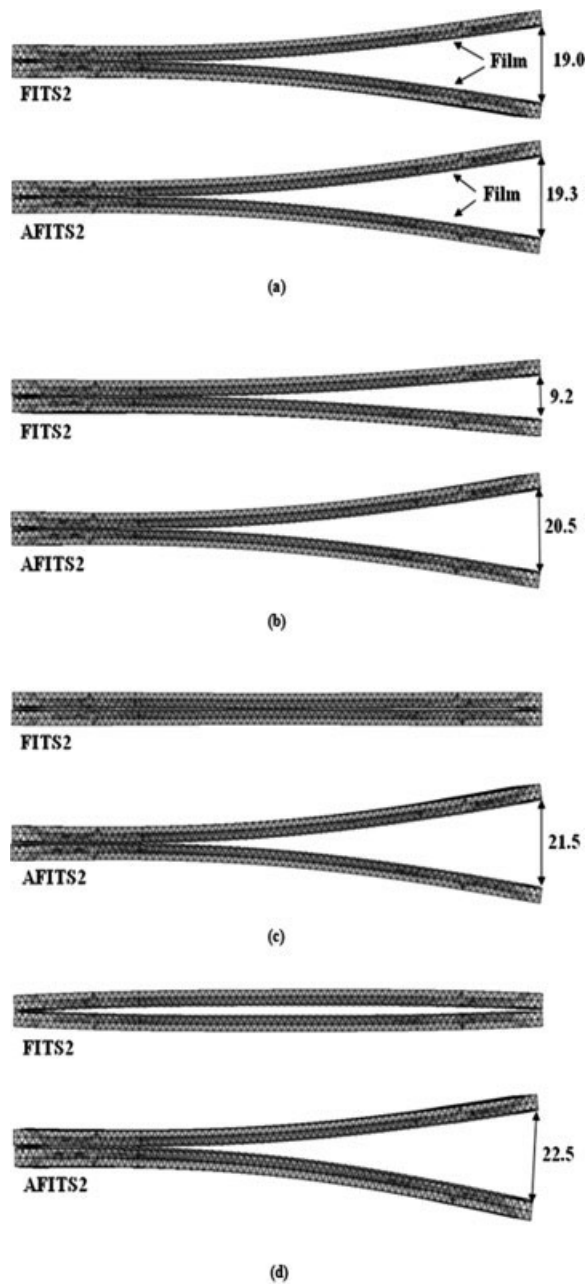


Figure 10 Predicted warpage of FITS2 and AFITS2 specimens numerically molded after ejection and annealing at 80°C with increasing annealing time: (a) after ejection, (b) for 10 min, (c) for 20 min, and (d) for 30 min.

to compressive mode during molding due to the solidification of injected hot resin.

Warpage of FITS2 and AFITS2 specimens after both ejection and annealing is shown in Figure 9 for various annealing time. FITS2 and AFITS2 specimens were bent after ejection in such a way that the film side was protruded. It was also observed in Figure 9(a) that the warpage of AFITS2 containing the annealed film which had been shrunk and relaxed sufficiently by the preannealing was larger than that of FITS2 after ejection. This behavior can be

explained by the fact that the unannealed film inserted into the FITS2 specimen was shrunk thermally by the hot injected resin during filling stage. As the two tensile specimens were annealed at 80°C, the gap between the two FITS2 specimens shown in the figure was decreased with increasing annealing time and the WRP occurred for annealing time between 10 and 20 min. After the WRP, the reversed gap between the two specimens was increased further as shown in Figure 9(d). However, on the contrary to the case of FITS2, the gap between the two AFITS2 specimens was not decreased after annealing and the WRP was not observed. Figure 10 shows the predicted warpage of FITS2 and AFITS2 specimens and it was almost similar to the experimental results. Numerical results indicated that application of proper thermal expansion coefficients to numerical analysis can describe the irreversible relaxation process of molecular orientation and the viscoelastic behavior of polymeric material can be represented by using a shift function based on the time temperature superposition theory. The numerical and experimental results indicate that the WRP is mainly caused by the combined effect of thermal shrinkage of the inserted film and relaxation of residual stresses in the film and the substrate during annealing.

CONCLUSIONS

Virgin injection molded specimens without the inserted film and FIM specimens with annealed or unannealed film were prepared by using an injection molding machine with a two-cavity mold. Full three-dimensional numerical analysis was also performed for FIM specimens. After the specimens were ejected from the mold, they were annealed at 80°C to investigate the thermoviscoelastic deformation and warpage of the FIM specimens. Both experimental and numerical results showed that the FIM specimen with unannealed film was bent such that the film side was protruded after ejection and it was gradually bent in the opposite direction during annealing. The “WRP” is caused by the combined effect of thermal shrinkage of the inserted film and relaxation of residual stresses in the specimen during annealing.

Molding experiments were conducted through collaboration with Korea Institute of Industrial Technology and Min Sung Precision Co. Ltd.

References

1. Leong, Y. W.; Kotaki, M.; Hamada, H. *J Appl Polym Sci* 2007, 104, 2100.
2. Leong, Y. W.; Ishiaku, U. S.; Kotaki, M.; Hamada, H. *Polym Eng Sci* 2006, 46, 1674.

3. Yamaguchi, S.; Leong, Y. W.; Tsujii, T.; Mizoguchi, M.; Ishiaku, U. S.; Hamada, H. *J Appl Polym Sci* 2005, 98, 294.
4. Leong, Y. W.; Yamaguchi, S.; Mizoguchi, M.; Hamada, H.; Ishiaku, U. S.; Tsujii, T. *Polym Eng Sci* 2004, 44, 2327.
5. Denizart, O.; Vincent, M.; Agassant, J. F. *J Mater Sci* 1995, 30, 552.
6. Lee, S. C.; Youn, J. R. *J Reinf Plast Comp* 1999, 18, 186.
7. Jung, J. H.; Lee, S. W.; Youn, J. R. *Macromol Symp* 1999, 148, 263.
8. Kramschuster, A.; Cavitt, R.; Ermer, D.; Chen, Z.; Turng, L-S. *Polym Eng Sci* 2005, 45, 1408.
9. Liao, S. J.; Hsieh, W. H. *Polym Eng Sci* 2004, 44, 2029.
10. Fan, B.; Kazmer, D. O.; Bushko, C.; Theriault, R. P.; Poslinski, A. J. *J Polym Sci Part B: Polym Phys* 2003, 41, 859.
11. Djurner, K.; Kubát, J.; Rigdahl, M. *Polymer* 1977, 18, 1068.
12. Kubát, J.; Rigdahl, M. *Polymer* 1975, 16, 925.
13. Kim, S. H.; Kim, C. H.; Oh, H.; Choi, C. H.; Kim, B. Y.; Youn, J. R. *Kores-Aust Rheol J* 2007, 19, 183.
14. Treuting, R. G.; Read, W. T., Jr. *J Appl Phys* 1951, 22, 130.
15. Kim, S. K.; Lee, S. W.; Youn, J. R. *Kores-Aust Rheol J* 2002, 14, 107.
16. Zoetelief, W. F.; Douven, L. F. A.; Ingen Housz, A. *J Polym Eng Sci* 1996, 36, 1886.
17. Hastenberg, C. H. V.; Wildervanck, P. C.; Leenen, A. J. H. *Polym Eng Sci* 1992, 32, 506.
18. Mathar, J. *Iron Steel* 1934, 56, 249.
19. Kim, C. H.; Youn, J. R. *Polym Test* 2007, 26, 862.
20. Kim, C. H.; Kim, S.; Oh, H.; Youn, J. R. *Fiber Polym* 2007, 8, 443.
21. Determining residual stresses by the Hole-Drilling Strain-Gage Method, *Annu Book of ASTM E837-01* 2001.
22. Measurement Group Tech Note TN-503-5 1996.
23. Wang, T.; Young, W. *Eur Polym J* 2005, 41, 2511.
24. Maxwell, A. S.; Turnbull, A. *Polym Test* 2003, 22, 231.
25. Sicot O.; Gong, X. L.; Cherouat, A.; Lu, J. *J Compos Mater* 2003, 37, 831.
26. Kabanemi, K. K.; Vaillancourt, H.; Wang, H.; Salloum, G. *Polym Eng Sci* 1998, 38, 21.
27. Schajer, G. S. *J Eng Mater-T ASME* 1988, 110, 338.
28. Flaman, M. T.; Manning, B. H. *Exp Mech* 1985, 25, 205.
29. Schajer, G. S. *J Eng Mater-T ASME* 1981, 103, 157.
30. Macosko, C. W.; *Rheology, Principles, Measurements, and Applications*; Wiley-VCH: New York, 1994.
31. Kennedy, P. *Flow Analysis Reference Manual*; Moldflow: Australia, 1993.
32. Santhanam, N.; Chiang, H. H.; Himasekhar, K.; Tuschak, P.; Wang, K. K. *Adv Polym Tech* 1991/1992, 11, 77.
33. Fldugge, W. *Viscoelasticity*; Springer-Verlag: New York, 1975.
34. *Analysis User's Manual Volume III: Materials*; ABAQUS Inc.: USA, 2003.